Microbiome

RESEARCH

Open Access

Microbial metabolism in laboratory reared marine snow as revealed by a multi-omics approach

Lei Hou[1†], Zihao Zhao[1,2†], Barbara Steger-Mähnert[2], Nianzhi Jiao[1*], Gerhard J. Herndl[2,3*] and Yao Zhang[1*]

Abstract

Background Marine snow represents an organic matter-rich habitat and provides substrates for diverse microbial populations in the marine ecosystem. However, the functional diversity and metabolic interactions within the microbial community inhabiting marine snow remain largely underexplored, particularly for specific metabolic pathways involved in marine snow degradation. Here, we used a multi-omics approach to explore the microbial response to laboratory-reared phytoplankton-derived marine snow.

Results Our results demonstrated a dramatic shift in both taxonomic and functional profiles of the microbial community after the formation of phytoplankton-derived marine snow using a rolling tank system. The changes in microbial metabolic processes were more pronounced in the metaproteome than in the metagenome in response to marine snow. Fast-growing taxa within the Gammaproteobacteria were the most dominant group at both the metagenomic and metaproteomic level. These Gammaproteobacteria possessed a variety of carbohydrate-active enzymes (CAZymes) and transporters facilitating substrate cleavage and uptake, respectively. Analysis of metagenome-assembled genomes (MAGs) revealed that the response to marine snow amendment was primarily mediated by *Alteromonas*, *Vibrio*, and *Thalassotalea*. Among these, *Alteromonas* exclusively expressing auxiliary activities 2 (AA2) of the CAZyme subfamily were abundant in both the free-living (FL) and marine snow-attached (MA) microbial communities. Thus, *Alteromonas* likely played a pivotal role in the degradation of marine snow. The enzymes of AA2 produced by these *Alteromonas* MAGs are capable of detoxifying peroxide intermediates generated during the breakdown of marine snow into smaller poly- and oligomers, providing available substrates for other microorganisms within the system. In addition, *Vibrio* and *Thalassotalea* MAGs exhibited distinct responses to these hydrolysis products of marine snow in different size fractions, suggesting a distinct niche separation. Although chemotaxis proteins were found to be enriched in the proteome of all three MAGs, differences in transporter proteins were identified as the primary factor contributing to the niche separation between these two groups. *Vibrio* in the FL fraction predominantly utilized ATP-binding cassette transporters (ABCTs), while *Thalassotalea* MAGs in the MA fraction primarily employed TonB-dependent outer membrane transporters (TBDTs).

[†]Lei Hou and Zihao Zhao contributed equally to this work.

*Correspondence:
Nianzhi Jiao
jiao@xmu.edu.cn
Gerhard J. Herndl
gerhard.herndl@univie.ac.at
Yao Zhang
yaozhang@xmu.edu.cn
Full list of author information is available at the end of the article

Conclusions Our findings shed light on the essential metabolic interactions within marine snow-degrading microbial consortia, which employ complementary physiological mechanisms and survival strategies to effectively scavenge marine snow. This work advances our understanding of the fate of marine snow and the role of microbes in carbon sequestration in the ocean.

Keywords Marine snow, Marine snow-degrading microbes, Free-living and marine snow-attached microbes, Metagenomics, Metaproteomics

Background

Marine snow, typically larger than 500 μm in size, is ubiquitous in the marine ecosystem, with its abundance ranging from 1 to 100 aggregates per liter [1, 2]. It constitutes more than 90% of the vertical flux of particulate organic matter to the deep ocean [3], being one key vector of the biological carbon pump. Marine snow is composed of complex components [1, 4]. Phytodetritus, referred to phytoplankton-derived organic matter, plays a predominant role in the formation of marine snow, accounting for the majority of the annual export of organic material from the euphotic to the oceanic deep waters [2]. It is well known that phytodetritus typically supports a large number of active microbes, leading to their crucial involvement in key biogeochemical processes such as secondary production, carbon utilization and degradation, and nutrient recycling [5, 6]. Marine snow also incorporates dead zooplankton and fecal pellets [2]. For instance, the compounds produced by gelatinous zooplankton have been found to episodically contribute to the export of organic matter to the deep ocean, serving as a substantial organic matter source for deep-sea microbes [7–10].

Microbial heterotrophic metabolism leads to the solubilization of marine snow. The microbes colonizing marine snow produce abundant extracellular enzymes, primarily highly active hydrolytic enzymes, to break down complex macromolecular organic components from the marine snow [6, 11–16], ultimately resulting in (in)organic matter-enriched plumes [11, 17]. Microbes lacking the capability to produce extracellular enzymes benefit from the release of these small molecular substrates [18]. Therefore, the marine snow-attached (MA) and free-living (FL, near the plume) microbial communities undergo both a structural and functional succession throughout the process of marine snow degradation [19–22]. Increasing evidence indicates that some specific heterotrophic microbial populations often exhibit a transient dominance in the degradation of phyto-organic matter, such as members of Gammaproteobacteria, Bacteroidetes, and the *Roseobacter* clade [23–26]. These microbial activities initiate the degradation of marine snow and significantly impact the fate of marine snow, ultimately influencing the efficiency of the biological carbon pump [11, 27–30].

The response of microbial communities to marine snow has been investigated through field and micro- and mesocosm experiments, revealing distinct successional patterns in dominant species and metabolism responding to phytoplankton blooms [31–35]. For example, it was observed that members of the Bacteroidetes (Flavobacteriia), Gammaproteobacteria, and Alphaproteobacteria (*Roseobacter* clade) rapidly responded to a phytoplankton bloom in the southern North Sea (German Bight) by upregulating carbohydrate-active enzymes (CAZymes) and various transporter proteins, allowing for the efficient breakdown of algal organic matter [33, 34, 36]. Within mesoscale eddy systems, driven by intensified phytoplankton primary production and enhanced organic carbon export, different members of Gammaproteobacteria, Bacteroidetes, Alphaproteobacteria, and Planctomycetes frequently emerged as dominant active taxa [37, 38]. In addition, a microcosm experiment supplemented with phytoplankton-derived dissolved organic matter (DOM) demonstrated the rapid proliferation of *Vibrio* (Gammaproteobacteria), followed by members of Flavobacteriia (Bacteroidetes), accompanied by a shift in extracellular enzyme activity [39]. These studies have advanced our understanding of microbial community structure and metabolism in response to phytoplankton production as well as marine snow formation across various marine provinces.

However, characterizing the changes in the taxonomic and functional profiles of MA and FL microbial communities during the degradation of marine snow is challenging due to the difficulty of capturing real-time response processes in the field. Therefore, there is still no consensus on how the dominant populations respond to marine snow and on the microbial metabolism on marine snow. In this study, we simulated marine snow formation with phytoplankton-derived aggregates using rolling tanks in an experimental setup [40]. We integrated the metagenomic and metaproteomic datasets to identify the key microbial players in marine snow degradation and to gain a comprehensive understanding of the underlying physio-ecological mechanisms and strategies of MA and FL microbes in response to marine snow.

Methods

Establishing a microbial culture system with phytoplankton-derived marine snow in rolling tanks

A non-axenic microalgae *Picochlorum* sp. was cultured in f/2 medium [41, 42] at ~ 25 °C under artificial solar radiation as described in Unanue et al. [43]. Cultures were sampled daily to measure the optical density (OD) at 550 nm using a spectrophotometer (Hitachi U-2000) until they reached the early stationary phase (Supplementary Fig. 1). Subsequently, the cultures were autoclaved and evenly transferred to three 5-L serum bottles. These bottles contained prefiltered (3-μm pore-size polycarbonate membrane, Millipore) natural seawater collected from the surface waters of the Adriatic Sea (43°N, 15°E). Two serum bottles were only filled with prefiltered natural seawater to serve as a control. All the bottles were placed on a rolling table in the dark at ~ 22.5 °C (Supplementary Fig. 2a, b, c) [40]. Phytoplankton-derived marine snow began to form in the rolling tanks within 2 h after autoclaved algae were added (Supplementary Fig. 2d, e, f), and the concentration of total organic carbon was estimated to be ~ 6.64 mM based on the optical density of algae cell (Supplementary Table 1) [44, 45].

Monitoring prokaryotic abundance in marine snow and ambient water

Samples for prokaryotic abundance in the three culture bottles were collected and counted every 3 to 4 h, while samples in the control bottles were collected and counted every ~ 10 h. For the free-living (FL) cells in the culture bottles, 1–2 mL particle-free ambient water was preserved with formaldehyde (final concentration of 2%) and stored at 4 °C. Similarly, for the total cells in the control bottles, 1–2 mL of water was treated using the same preservation method. For the marine snow-attached (MA) cells in the culture bottles, visible aggregates, extensively colonized by microbial cells, were randomly collected. The aggregates were then pre-treated to obtain cell suspensions, following the procedures described by Agis et al. [46] and Besemer et al. [47, 48] with some modifications. Briefly, approximately 20 μL of visible particles (containing both the particulate fraction and its porewater) was dispersed in 0.5–1 mL tetrasodium pyrophosphate solutions (final concentration of 25 μM) for 1 h. Subsequently, the samples were sonicated (40 W) at room temperature for 3 min using an ultrasonic water bath. Cell suspensions free of particles were then transferred to a new tube and preserved using the same method as described above.

For the enumeration of the FL cell abundance, fixed water samples were filtered through polycarbonate membranes with pore sizes of 0.8 μm and then 0.22 μm (25-mm diameter, Millipore) at a pressure of < 0.03 MPa. The harvested cells within the size range of 0.22–0.8 μm were then counted. For the enumeration of the MA microbes and of microbes in the control tanks, fixed water samples were directly filtered onto 0.22-μm pore-size polycarbonate membranes (25-mm diameter, Millipore) at a pressure of < 0.03 MPa. Microbial cells were stained with 4′,6-diamidino-2-phenylindole (DAPI) [49] at a final concentration of 2 μg mL^{-1}, and the cells were counted using a Zeiss Axio Imager M2 epifluorescence microscope.

Nucleic acid and protein extraction

Once prokaryotic cells reached the early stationary phase after about 30 h, the marine snow suspension in the rolling tanks was filtered through 3-μm and then 0.22-μm pore-size polycarbonate membranes (47-mm diameter, Millipore) at a pressure of < 0.03 MPa to obtain the MA community (size fraction: > 3 μm) and FL community (size fraction: 0.22–3 μm) for further analysis. Water samples in the control bottles were filtered directly through 0.22-μm pore-size polycarbonate membranes (47-mm diameter, Millipore) at a pressure of < 0.03 MPa to obtain the control community. A total of eight samples for metagenomic and metaproteomic analyses were collected from the control tanks (two biological replicates), the FL (three biological replicates), and the MA (three biological replicates) microbial community.

Nucleic acid extraction was carried out using the modified phenol-chloroform-isoamyl alcohol method [50]. Briefly, membranes were cut into small pieces, transferred into tubes (2-mL volume) containing beads and lysis buffer (100-mM EDTA, 50-mM Tris, and 0.75-M sucrose), and then homogenized using the MP FastPrep-24 instrument (MP Biomedicals). The homogeneous liquid samples were digested with lysozyme, proteinase K, and sodium dodecyl sulfate. Nucleic acids were extracted from the lysates with NaCl (5 M) and phenol-chloroform-isoamyl alcohol (25:24:1). Residual phenol was removed using chloroform-isoamyl alcohol (24:1), and the nucleic acids were precipitated, collected, and cleaned using ice-cold isopropanol and 70% ethanol. Concentration and purity of nucleic acid extracts were quantified and analyzed using Quant-iT™ PicoGreen™ dsDNA Assay Kit (Invitrogen) and a NanoDrop ND-1000 spectrophotometer, respectively.

Protein extraction was carried out according to Dong et al. [51] and Zhao et al. [8] with some modifications. Briefly, membranes were cut into small pieces and suspended in ~ 5-mL lysis buffer containing urea (7 M), thiourea (2 M), dithiothreitol (DTT, 1%), 3-[(3-cholamidopropyl)-dimethylammonium]-1-propanesulfonate (CHAPS, 2%), and protease inhibitor cocktail. The suspension was shaken and homogenized using a Vortex-Genie 2 mixer with a vortex adapter (MO BIO)

at moderate speed for 12 h at room temperature and then centrifuged at 7500 × *g* for 15 min at room temperature to separate the supernatant from the membrane pieces. The supernatant was concentrated using a 3000-Da Amicon Ultra-15 Centrifugal Filter Unit (Millipore), and the protein concentrations were determined using a Pierce 660-nm Protein Assay (Thermo Fisher Scientific). The protein solution was subjected to two methods of digestion, in-gel and in-solution trypsin digestions (1:100, w/w), and then incubated at 37 °C overnight. After digestion, the peptides were processed into freeze-dried powders. The freeze-dried powders were then resuspended in 1% (final concentration) trifluoroacetic acid (TFA) and desalted using C18 Tips (Thermo Fisher Scientific).

Metagenomic sequencing, assembly, and annotation

The nucleic acid extracts were sent to Microsynth AG, Switzerland, for sequencing. Reads from each metagenomic dataset were individually assembled using MEGAHIT (v1.1.2) [52] with default settings. Putative genes were then predicted on contigs longer than 200 bp using Prodigal (2.6.3) [53] in metagenome mode (−p meta). The abundance (RPKM) of each predicted gene was evaluated by mapping the reads back using the BWA algorithm (0.7.16a) [54]. For all the predicted genes, function annotation was performed using the eggNOG database (v5.0) [55] via eggNOG-mapper [56], clusters of orthologous genes (COG) database [57], and Kyoto Encyclopedia of Genes and Genomes (KEGG) database [58]. The taxonomic affiliation of sequences was determined using the lowest common ancestor algorithm adapted from DIAMOND (0.8.36) [59], by performing a search against the nonredundant (NR) database. The taxonomic determination was based on the top 10% hits with an *e*-value < 1×10^{-5} (−top 10).

For CAZymes, the genes were annotated using hmmsearch against the dbCAN database (*e*-value < 1×10^{-10}, coverage > 0.3) [60]. KO groups such as K00026, K00055, K00108, K11517, K18370, and K19511 were manually checked and classified as AAs of CAZymes according to function description and EC numbers. SignalP (4.0) was used to detect the presence of signal peptides for bacterial sequences [61]. For TBDTs, substrate specificity was predicted by searching (blastp) TBDTs against a curated TBDT sequence database of pure cultures with a threshold of identify ≥ 30% [62].

Metagenome-assembled genomes (MAGs) construction

Reads were co-assembled using MEGAHIT (v1.1.2) [52] to construct metagenome-assembled genomes (MAGs). The contigs were clustered using two separate automatic binning algorithms: MaxBin [63] and MetaBAT [64]. The generated bins were automatically dereplicated and aggregated using Metawrap [65]. Bins meeting the criteria of ≥ 50% completeness and < 10% contamination were retained for further analysis. In total, 17 MAGs exhibited a completeness of greater than 90% with less than 5% contamination (MIMAGs category of "high quality" or "near complete"), and 60 MAGs showed a completeness of 50–90% with contamination < 10% (MIMAGs category of "medium quality"). Short reads from each metagenome were mapped to the bins using the BWA algorism (0.7.16a) [54]. Gene prediction for each bin was performed using Prodigal (2.6.3) [53]. Gene annotation was performed using KofamKOALA [58].

Phylogenomic analysis

The multiple sequence alignment (MSA) from the 77 prokaryotic MAGs (high and medium quality) was produced by the Genome Taxonomy Database toolkit (GTDB-TK) [66]. The phylogenomic tree of MSA was then constructed using RAxML (version 8.2.12) under all-in-one analysis mode (LG + G8 + F) [67]. The visualization was carried out using the Interactive Tree of Life (http://itol.embl.de/) [68].

Metaproteomic analysis, identification, annotation, and quantification

The peptides were analyzed using a Q-Exactive Hybrid Quadrupole-Orbitrap mass spectrometer (Thermo Scientific). The MS/MS spectra from each proteomic sample were searched against the protein database from the total community and each bin using SEQUEST-HT engines [69]. The resulting matches were further validated using Percolator in Proteome Discoverer 2.1 (Thermo Fisher Scientific). To minimize the probability of false peptide identification, the target–decoy approach [70] was employed. Only results with a peptide-level false discovery rate (FDR) < 1% were retained. For protein identification, a minimum of two peptides and at least one unique peptide were required. Protein quantification was conducted using a label-free quantitative method based on chromatographic peak area [71]. The metaproteomic results of each sample are shown in Supplementary Table 2.

Statistical analysis and visualization

Paired and unpaired *t*-test and nonparametric Wilcoxon tests were used to compare two variables because normal distribution of the individual data sets was not always met. The differentially expressed proteins (DEPs) among size fractions for each MAG were identified using edgeR ($|\log_2 FC| \geq 1$, adjusted *P*-value < 0.05). Nonmetric multidimensional scaling (NMDS) analysis was used to assess the similarity between samples based on Bray–Curtis similarities using PRIMER v5 software [72]. Similarity tests

for differences between samples were performed using a one-way analysis of similarity (ANOSIM) [72]. Other statistical analyses, including α-diversity (Shannon index), Bray–Curtis dissimilarity, and PERMANOVA analysis, were performed using the vegan package in *R*. Data visualization was performed using SigmaPlot v12.5, as well as the ggplot2 and ComplexHeatmap packages in *R*.

Results

Structure and function of MA and FL prokaryotic communities in the marine snow culture system

The prokaryotic abundances in the marine snow culture system showed that the total community entered early stationary phase after approximately 30 h, reaching abundances of ~ 4.7×10^7 and ~ 3.3×10^9 cells mL^{-1} for the FL and MA communities, respectively. The number of prokaryotes in the control treatment (without marine snow addition) remained nearly constant ($4.9–8.6\times10^6$ cells mL^{-1}) (Supplementary Fig. 3).

The community structure, taxonomic diversity, and functional variability were examined through combined metagenomic and metaproteomic analyses. The α-diversity of both taxonomic (unpaired *t*-test, $P<0.01$) and functional (unpaired *t*-test, $P<0.05–0.01$) composition in the metaproteomes was significantly higher compared to the results obtained from the metagenomes, except for the taxonomic composition of the MA community (Fig. 1a, b, Supplementary Table 3). The FL community exhibited lower α-diversity in taxonomic composition compared to the MA community in the metaproteomes (unpaired *t*-test, $P<0.05$; Fig. 1a, Supplementary Table 3) but displayed higher α-diversity than the MA community at functional levels in both the metagenomes and metaproteomes (unpaired *t*-test, $P<0.01$; Fig. 1b, Supplementary Table 3). The Bray–Curtis dissimilarity indicated a significantly higher degree of taxonomic variation between the FL and MA fraction in the metagenomes than the metaproteomes (unpaired *t*-test, $P<0.01$; Fig. 1c), whereas the metaproteomes exhibited greater functional versatility (unpaired *t*-test, $P<0.01$; Fig. 1d). This observation suggests a more variable expression of proteins/enzymes within the microbial community in response to the addition of marine snow. The functional annotations at the COG level further support this observation. In the metagenomes, despite shifts in both taxonomic and functional profiles observed in both the FL and MA fractions following marine snow amendment compared to the control, the changes in

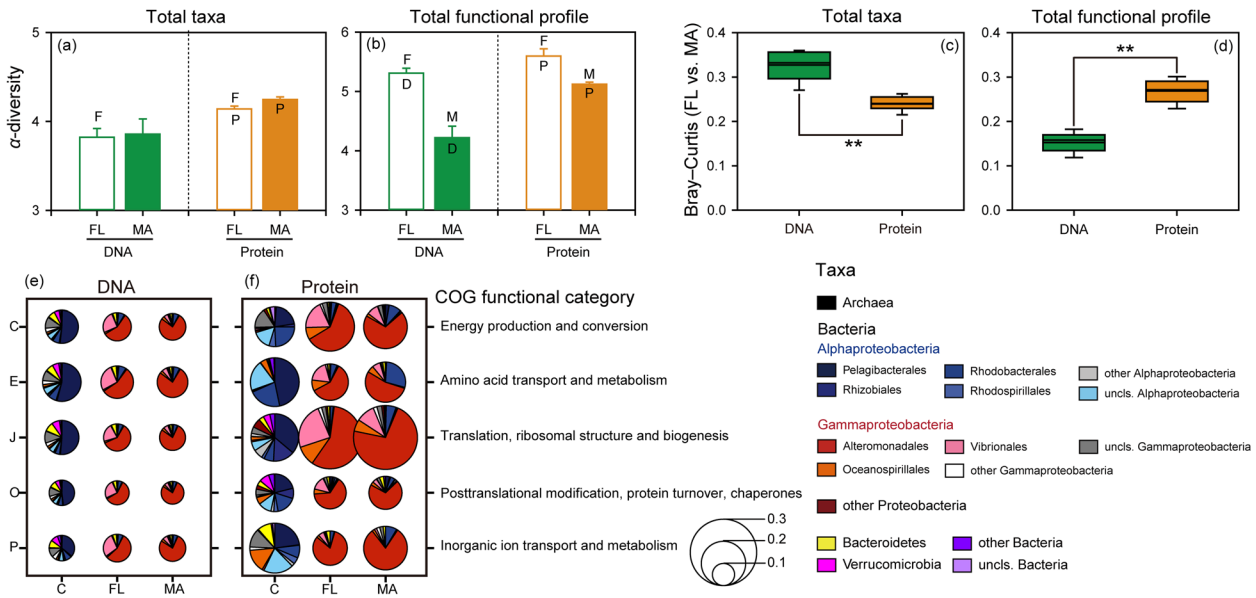

Fig. 1 Taxonomic and functional profile of free-living (FL) and marine snow-attached (MA) communities in the marine snow culture system. **a** Alpha-diversity (Shannon index) of taxonomic and **b** functional composition in the FL and MA communities at both the gene and protein levels. F, significant difference in the FL fraction between the gene and protein levels ($P<0.05–0.01$); M, significant difference in the MA fraction between the gene and protein levels ($P<0.01$); D, significant difference in the metagenome between the FL and MA communities ($P<0.01$); P, significant difference in the metaproteome between the FL and MA communities ($P<0.05–0.01$). **c** Bray–Curtis dissimilarity in taxonomy and **d** function between the FL and MA communities at both the gene and protein levels. The boxes show the mean, median, and interquartile range (IQR); the whiskers show 1.5 times the IQR of the lower and upper quartiles or the data range. $^{**}P<0.01$. **e** Scatter pie charts showing the compositions and relative abundances of the gene- and **f** protein-based taxonomic contribution to the major functions, including C, E, J, O, and P categories, based on the Clusters of Orthologous Groups (COGs) database at the phylum level (order level for Alpha- and Gammaproteobacteria and class level for other proteobacteria). C, control community

relative abundances of COG categories were low (Fig. 1e, Supplementary Fig. 4a, c, Supplementary Fig. 5a, Supplementary Data 1).

In contrast, in the metaproteomes, significant differences were observed for the following COG functional categories: energy production and conversion (C), translation, ribosomal structure and biogenesis (J), posttranslational modification, protein turnover, chaperones (O), and inorganic ion transport and metabolism (P) following marine snow amendment (PERMANOVA, $P < 0.01$; Fig. 1f, Supplementary Fig. 4b, d, Supplementary Fig. 5b, Supplementary Data 1). The relative abundance of proteins involved in amino acid transport and metabolism (E) showed distinct differences between the FL and MA communities (Fig. 1f, Supplementary Fig. 5b). Both the metagenomes and metaproteomes indicated a shift in community dominance from Alphaproteobacteria to Gammaproteobacteria following the addition of marine snow. Specifically, more than 84% of the prokaryotes in both the FL and MA communities belonged to the orders Alteromonadales, Vibrionales, and Oceanospirillales. In addition, Rhodobacterales became the dominant alphaproteobacterial taxon after marine snow addition, while Pelagibacterales, which originally dominated the community, became rare (Fig. 1e, f, Supplementary Fig. 5).

Furthermore, clustering the proteins into KEGG Orthology (KO) groups revealed that the addition of marine snow resulted in highly expressed proteins/enzymes observed in specific functional categories, including auxiliary activities (AAs) of CAZyme subfamilies, transporters, two-component pathways, biofilm formation, oxidative phosphorylation, and ribosomes. Notably, AAs and transporters were found to be overexpressed in the MA compared to the FL community (paired *t*-test, $P < 0.05$; Fig. 2, Supplementary Data 2). These results align with the higher Bray–Curtis dissimilarity (β-diversity) between FL and MA communities observed in the overall functional profiles of the metaproteomes compared to the metagenomes (Fig. 1d), providing further support for the hypothesis that a specific set of key proteins/enzymes drives the microbial community response to environmental perturbations, such as marine snow amendment. Pronounced changes in these key proteins/enzymes revealed by the metaproteomics analysis may be overlooked if solely analyzing metagenomes.

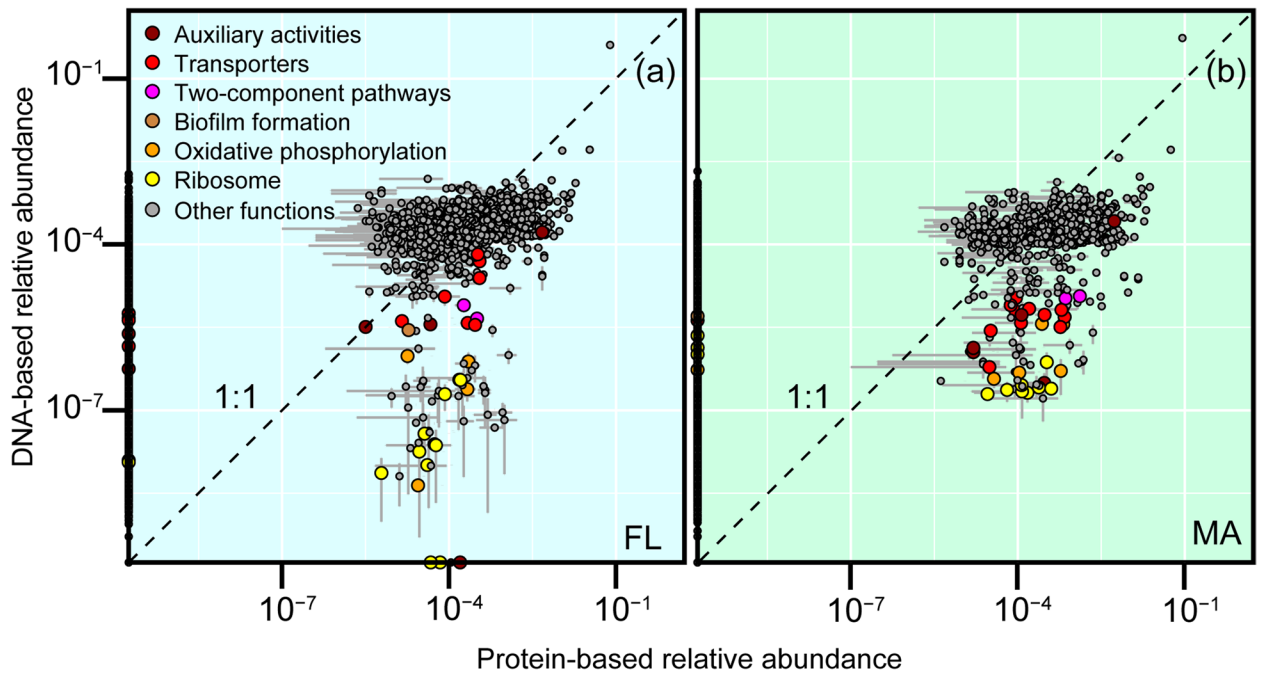

Fig. 2 Relationship between the relative abundance of genes and protein expression of KEGG Ontology (KO) groups. **a** Relationships in the free-living (FL) community. **b** Relationships in the marine snow-attached (MA) community. Dashed lines are the 1:1 line. The shadow lines represent error bars derived from three biological replicates in both FL and MA treatments. Some error bars are not visible because they are too small and fall within the boundaries of the dots

Characteristics of marine snow degradation as revealed by essential proteins

The relative abundances of AAs, ATP-binding cassette transporters (ABCTs), and TonB-dependent outer membrane transporters (TBDTs) were higher at the protein compared to the gene level, indicating a preference for the expression of CAZymes and transporter proteins as a response to marine snow amendment (Fig. 2, Supplementary Data 2). These enzymes/proteins primarily facilitate the microbial community in the degradation of algal debris and assimilation of substrates [6, 8, 9, 18, 73]. Therefore, we analyzed the taxonomic and functional composition of CAZymes and transporters. The taxonomic α-diversity of genes encoding CAZymes and transporters was higher in the MA community in both metagenomes and metaproteomes (unpaired t-test, $P < 0.01$; Fig. 3a, Supplementary Table 4). However, the functional α-diversity showed an opposite pattern, with the FL community exhibiting a higher α-diversity (unpaired t-test, $P < 0.01$; Fig. 3b, Supplementary Table 4). In addition, the taxonomic and functional α-diversity of CAZymes and transporter proteins

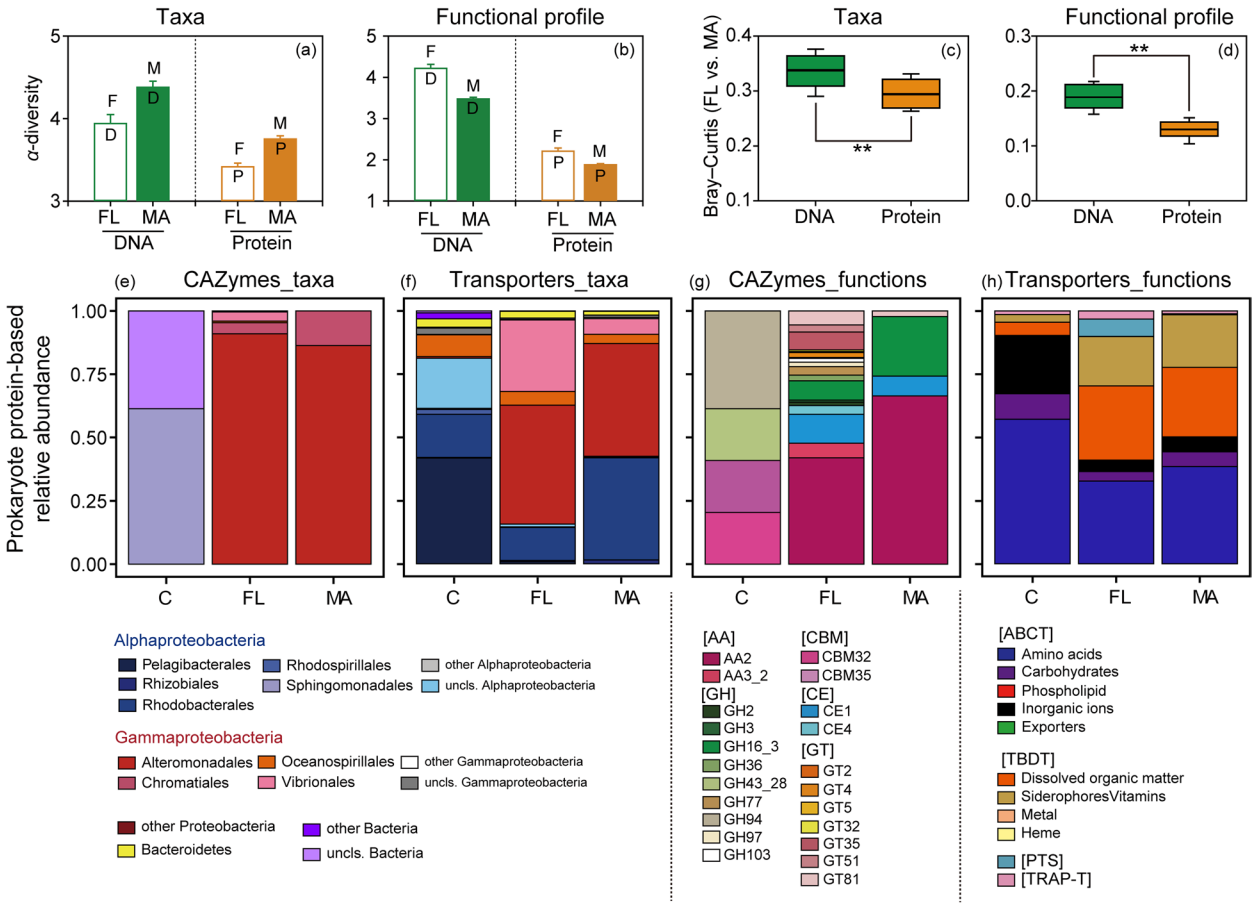

Fig. 3 Taxonomic and functional profile of carbohydrate-active enzymes (CAZymes) and transporter proteins in free-living (FL) and marine snow-attached (MA) communities in the marine snow culture system. **a** Alpha diversity (Shannon index) of taxa and **b** functions of CAZymes and transporter proteins in free-living (FL) and marine snow-attached (MA) communities at both the gene and protein levels. F, significant difference in the FL fraction between the gene and protein levels ($P < 0.01$); M, significant difference in the MA fraction between the gene and protein levels ($P < 0.01$); D, significant difference in the metagenome between the FL and MA communities ($P < 0.01$); P, significant difference in the metaproteome between the FL and MA communities ($P < 0.01$). **c** Bray–Curtis dissimilarity in taxa and **d** functions of CAZymes and transporter proteins between the FL and MA communities at both the gene and protein levels. The boxes show the mean, median, and interquartile range (IQR); the whiskers show 1.5 times the IQR of the lower and upper quartiles or the data range. $^{**}P < 0.01$. **e** Bar charts showing the taxonomic composition and relative abundance of CAZymes and **f** transporters at the phylum level (order level for Alpha- and Gammaproteobacteria and class level for other proteobacteria). **g** Stack bar charts showing the functional composition and relative abundance of CAZymes and **h** transporters. AA, auxiliary activity; CBM, carbohydrate-binding module; CE, carbohydrate esterase; GH, glycoside hydrolase; GT, glycosyl transferase. ABCT, ATP-binding cassette transporter; TBDT, TonB-dependent transporters; PTS, phosphotransferase system; TRAP-T, tripartite ATP-independent periplasmic transporter. C, control community

was consistently higher in the metagenomes compared to the metaproteomes (unpaired *t*-test, $P < 0.01$; Fig. 3a, b, Supplementary Table 4) in stark contrast to the overall taxonomic and functional α-diversity (Fig. 1a, b, Supplementary Table 3). The decreased diversity in CAZyme and transporter proteins in the metaproteome indicates that although most of the microbes carries corresponding genes, the expression was dominated by certain taxonomic groups that likely played a leading role in marine snow degradation. It is also notable that the resolution of mass spectrometry-based metaproteomic analysis is lower than metagenomic sequencing, leading to an underestimation of α-diversity at the protein level. The Bray–Curtis dissimilarity in both taxonomic and functional composition of genes encoding CAZymes and transporters between the FL and MA communities was higher in the metagenomes compared to the metaproteomes (unpaired *t*-test, $P < 0.01$; Fig. 3c, d).

Compared to the control, pronounced shifts were observed in the taxonomic composition of prokaryotes expressing CAZymes and transporters after the marine snow addition as revealed by the metaproteomes (Fig. 3e, f, Supplementary Fig. 6a, b). Alteromonadales and Chromatiales (Gammaproteobacteria) became the dominant groups, accounting for 95% and 100% of the total CAZymes in the FL and MA communities, respectively (Fig. 3e). CAZymes with AAs accounted for 48% and 66% of total CAZymes in the marine snow culture system in the FL and MA communities, respectively (Fig. 3g). We further categorized CAZymes into two types, namely periplasmic (cell-associated) and cytoplasmic (intracellular) enzymes, based on the presence of signal peptides [8, 74]. The results indicated that the AA2 enzymes (class II peroxidase) were predominantly located in the periplasmic space, constituting 79% and 75% of the periplasmic CAZymes in the FL and MA communities, respectively (Supplementary Table 5a). Glycosyl transferase (GT) was more abundant in the cytoplasmic than the periplasmic space (Supplementary Table 5). Moreover, a wide variety of CAZyme subfamilies was found in the cytoplasmic space of the FL community, in comparison to those in the MA community (Supplementary Table 5b). The relative abundance of cytoplasmic CAZymes in the FL community was also significantly higher than that in the MA community (Wilcoxon rank-sum test, $P < 0.05$; Supplementary Table 5b).

TBDTs were the major transporters utilized by microbes for substrate assimilation, constituting approximately 49% of the total transporter proteins in both the FL and MA communities after the addition of marine snow (Fig. 3h). The dominant taxonomic groups expressing TBDTs in both the FL and MA communities were members of Alteromonadales, with minor contributions from Rhodobacterales (1.8% in the FL and 3.3% in the MA community) and Bacteroidetes (5.4% in the FL and 3.1% in the MA community, Supplementary Fig. 6b). Substrate specificity analysis showed that TBDTs were predominantly involved in the uptake of DOM, contributing to 60% in the FL community and 57% in the MA community while also contributing to the uptake of iron-rich substrates (Supplementary Fig. 6d). ABCTs, as the prevalent and abundant transporters, exhibited relatively high expression levels in the control (90%) but decreased after marine snow addition (41% in FL and 50% in MA; Fig. 3h). These decreases coincided with a taxonomic shift from Pelagibacterales to Vibrionales and Rhodobacterales (Fig. 3f, Supplementary Fig. 6a). Substrates of ABCTs primarily included monomers such as amino acids, carbohydrates, and inorganic ions (Fig. 3h, Supplementary Fig. 6c). In addition, the phosphotransferase system (PTS) transporters and tripartite ATP-independent periplasmic transporters (TRAP-Ts) were also identified in the FL communities, comprising 7% and 3.2% of the total transporter proteins, respectively (Fig. 3h). Notably, all PTS transporters were found to originate from the Vibrionales.

Furthermore, two-component (signal transduction) pathways (TCPs) and bacterial secretion systems (BSSs) were also examined, as they have been shown to play important roles in marine snow degradation [31]. TCPs are implicated in mediating the response of bacteria to external stimuli, and BSSs are implicated in competing with nearby microorganisms [75, 76]. In the marine snow culture system, the taxonomic and functional compositions of TCPs and BSSs changed significantly compared to the control following the addition of marine snow (Supplementary Fig. 7). The major TCPs in both the FL and MA communities included proteins involved in the osmolarity response regulator protein R (OmpR) family, nitrogen regulation protein NR(I) (NtrC) family, chemotaxis (CheA) family, and polar flagellar synthesis and redox response (Supplementary Fig. 7 g, h, i, j, k), while the major BSSs consisted of proteins involved in the Type I secretion system (T1SS) and general secretion (Sec) pathways (Supplementary Fig. 7 l). The main group expressing these proteins was Alteromonadales in both the FL and MA fractions, and, in addition, Vibrionales in the FL community also significantly expressed these proteins (Supplementary Fig. 7a, b, c, d, e, f).

Phylogenetic affiliation and protein expression of dominant prokaryotic MAGs degrading marine snow

To identify the key bacteria degrading marine snow, we performed metagenomic co-assembly analysis and recovered 77 MAGs. These MAGs were grouped into five clades based on phylogenetic analysis, including

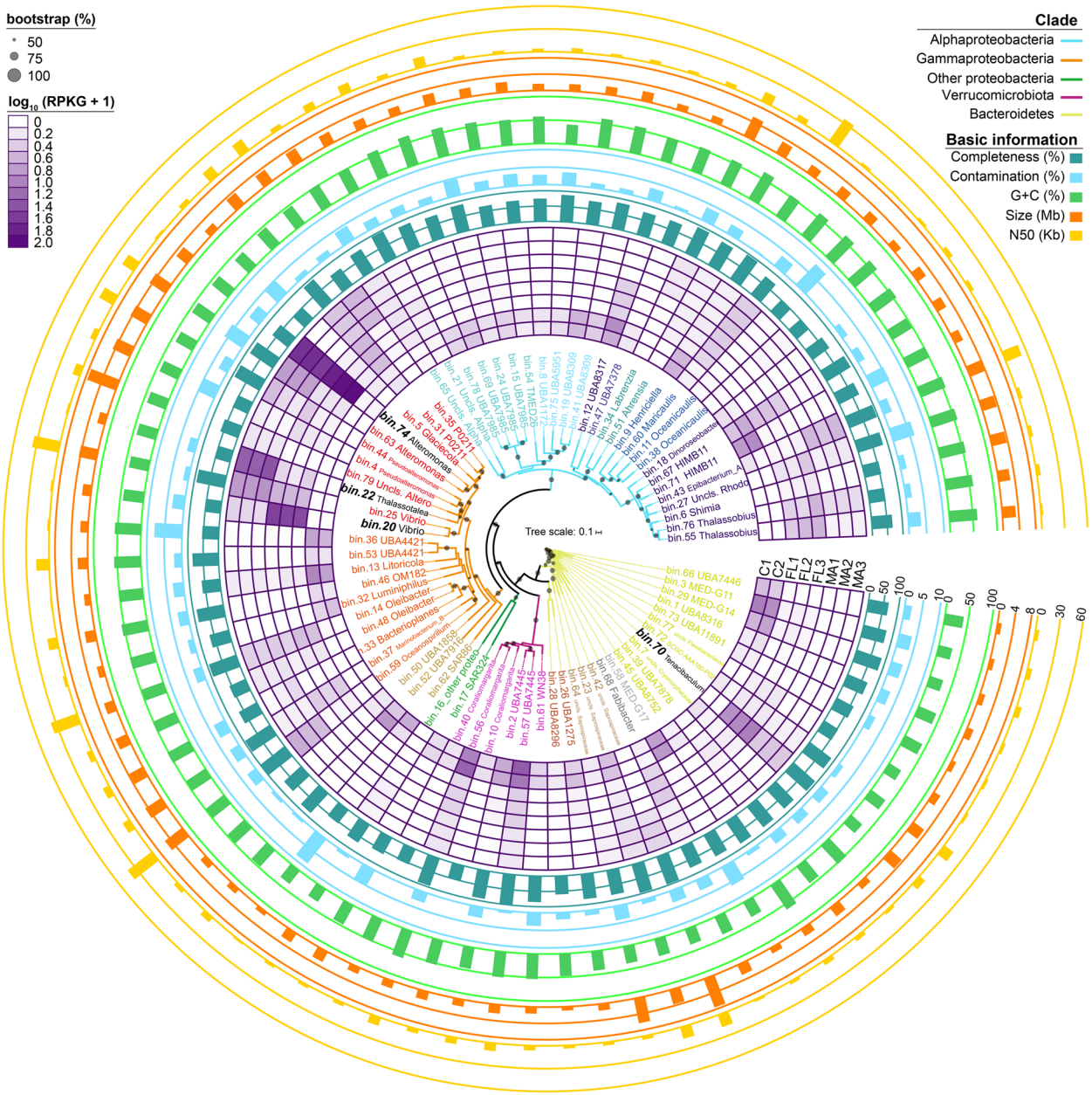

Fig. 4 Phylogenomic placement of the 77 prokaryotic metagenome-assembled genomes (MAGs) recovered in the marine snow culture system. Five main clades affiliated with Alphaproteobacteria (blue), Gammaproteobacteria (orange), other Proteobacteria (green), Verrucomicrobiota (pink), and Bacteroidetes (yellow) are indicated by differently colored fonts. Dominant MAGs are shown in black bold italics. The log-transformed reads per kilobase per genome (RPKG) values of prokaryotic MAGs in each sample are shown in the heatmap. The basic information, including completeness (cyan), contamination (blue), G + C (green), size (orange), and N50 (yellow), is shown in the bar chart. Bootstrap values ≧ 50% are shown in the phylogenetic tree by gray circles; the size of the circle corresponds to the magnitude of the bootstrap value. The scale bar represents the average number of amino acid substitutions per site. C, control; FL, free-living community in the marine snow micrcosm; MA, marine snow-attached community in the marine snow microcosm

Alphaproteobacteria, Gammaproteobacteria, Verrucomicrobiota, and Bacteroidetes (Fig. 4). By mapping the metagenomic reads back to the MAGs, we observed a niche separation among the MAGs. Three MAGs (bin.74, bin.22, and bin.20) belonging to Gammaproteobacteria showed the highest abundance in the marine snow culture system, surpassing that found in the control by two to three orders of magnitude (Fig. 4, Supplementary Fig. 8, Supplementary Data 3, Supplementary Data 4). Bin.74, bin.22, and bin.20

were further identified as members of the genera *Alteromonas*, *Thalassotalea*, and *Vibrio*, respectively. Among them, bin.74 was the most abundant, accounting for 52% and 42% of the reads mapped to all MAGs in the marine snow culture system for the FL and MA communities, respectively (Supplementary Data 4). Bin.20 exhibited a preference for the FL community, representing 20% of the reads mapped to all MAGs, whereas bin.22 showed a higher abundance in the MA community with 19% (Supplementary Data 4). The three MAGs exhibited a disproportionate increase compared to the control and became the predominant species by presumably assimilating substrate from phytoplankton-derived marine snow. In addition, another MAG, bin.70, identified as a member of the genus *Tenacibaculum* affiliated with Bacteroidetes, also exhibited an increase after marine snow addition accounting for 5% and 2% of the reads mapped to all MAGs in the FL and MA communities, respectively (Supplementary Data 4). The relative abundance of other prokaryotic clades, such as most members of Alphaproteobacteria and Verrucomicrobiota, experienced a significant decrease after marine snow addition (Fig. 4, Supplementary Fig. 9).

By integrating metaproteomic expressions with the functional profiles of key MAGs (bin.74, bin.22, and bin.20), we identified a distinct set of key enzymes/proteins expressed by each bacterium in response to marine snow addition. Thirty-eight to 49 proteins were found to be differentially expressed across the three bins (Fig. 5a, b, c). In bin.74 (*Alteromonas*), functional proteins associated with outer membrane receptor proteins, ribosomal proteins, and flagellin were upregulated (adjusted *P*-value < 0.05) in the FL and MA communities during

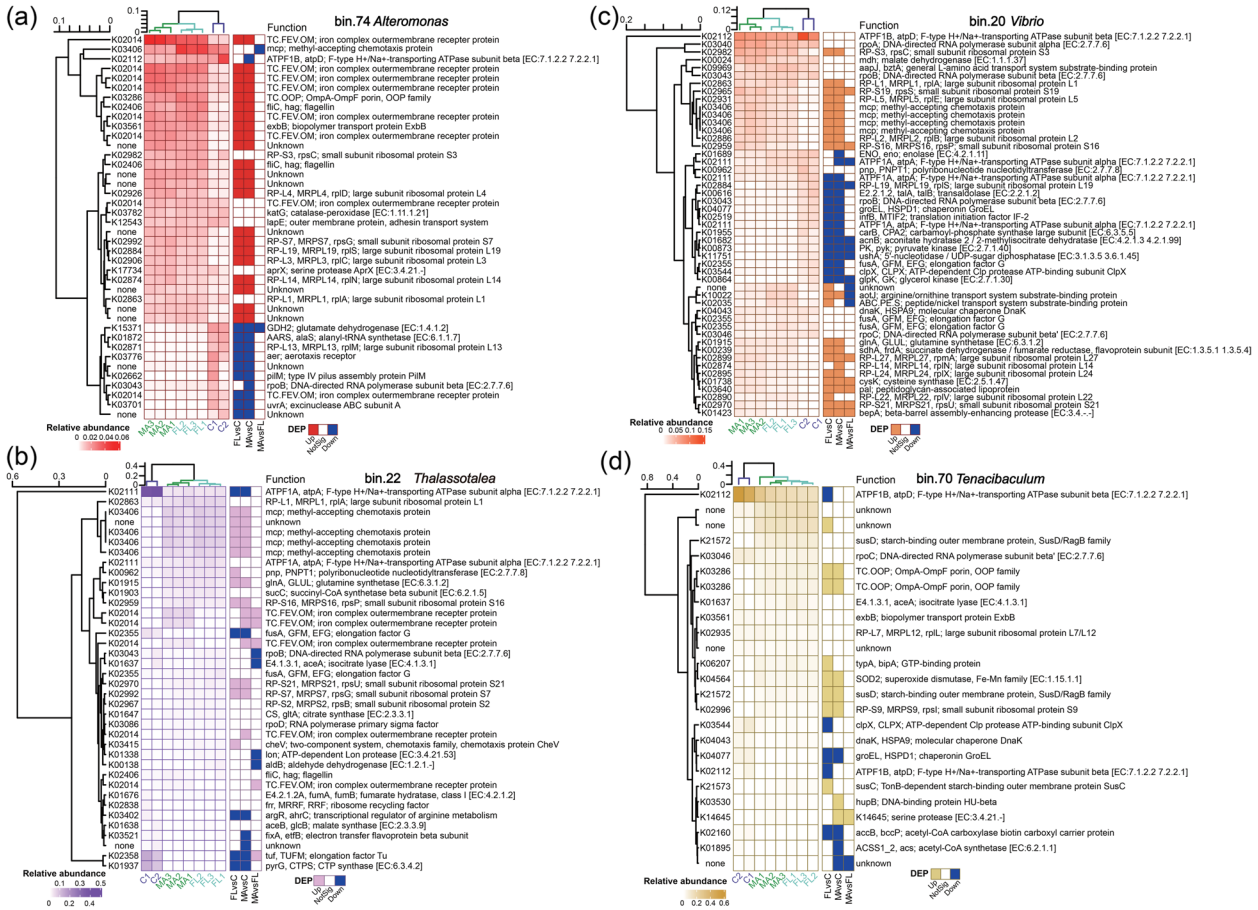

Fig. 5 Heatmaps protein expression pattern of the dominant taxa (**a** bin.74, **b** bin.22, **c** bin.20, and **d** bin.70) involved in marine snow degradation across each sample. The expression data represent the relative abundance over the proteome associated with each of the metagenome-assembled genomes (MAGs). The expressed proteins in each MAG with a relative abundance > 1% in at least one sample are shown. The colors carmine (bin.74), purple (bin.22), orange (bin.20), and yellow (bin.70) represent upregulated proteins (adjusted *P*-value < 0.05); the colors blue and white represent downregulated proteins (adjusted *P*-value < 0.05) and nonsignificantly regulated proteins, respectively. DEP, differentially expressed protein among size fractions for each MAG

growth in the marine snow culture system as compared to the control. This indicates a strong metabolic response of *Alteromonas* members to marine snow. Flagellin can help microbial colonization on particles, and the outer membrane proteins facilitate substrate uptake, which boost cellular metabolism such as protein synthesis, as reflected by the upregulation in ribosomal proteins [31, 73, 77]. These proteins were predominant in both FL and MA fractions. We also found that the catalase-peroxidase (KatG) was the only CAZyme detected at the protein level in bin.74 in all treatments, while it was absent in other bins (Fig. 5a). Methyl-accepting chemotaxis protein (MCP) displayed a notable upregulation in the FL compared to the MA fraction ($Log_2FC = 1.29$, adjusted *P*-value < 0.01) and control treatment ($Log_2FC = 0.74$, adjusted *P*-value < 0.05; Fig. 5a). KatG belongs to the AA2 of the CAZyme subfamily and plays an important role in detoxification of peroxide intermediates generated during the degradation of marine snow [78], whereas MCPs serve as primary chemoreceptors in prokaryotes, facilitating to sense environmental conditions, and move away from toxic chemicals [79]. Therefore, the characteristics exhibited by these two proteins of bin.74 in response to marine snow addition may contribute to its predominance in the marine snow culture system.

Bin.22 (*Thalassotalea*) exhibited a preference for the MA fraction, as indicated by both metagenomic and metaproteomic analyses (Fig. 4, Supplementary Table 6, Supplementary Data 4). Specifically, iron complex outer membrane receptor proteins (TC.FEV.OM), as one type of TBDT proteins facilitating the uptake of diverse compounds, were observed to be notably upregulated in the MA compared to FL fraction ($Log_2FC = 2.99 \sim 3.81$, adjusted *P*-value < 0.01) and the control treatment ($Log_2FC = 3.09 \sim 5.97$, adjusted *P*-value < 0.05; Fig. 5b). Additionally, proteins involved in chemotaxis, ribosomal proteins, DNA synthesis and replication, and amino acid synthesis were found to be upregulated (adjusted *P*-value < 0.05) in both FL and MA communities during growth in the marine snow culture system as compared to the control. These results from bin.22 also indicate a pronounced proliferation benefiting from marine snow, akin to bin.74.

Bin.20 (*Vibrio*) was predominantly found in the FL fraction (Fig. 4, Supplementary Table 6, Supplementary Data 4) and displayed a distinct functional expression pattern compared to bin.74 and bin.22. After the marine snow addition, proteins involved in chemotaxis, ABC transporters, amino acid synthesis, carbohydrate metabolism, and ribosomal proteins were upregulated in both the FL and MA fractions (adjusted *P*-value < 0.05; Fig. 5c). The upregulation of these proteins suggests that *Vibrio* may have enhanced the metabolism of low-molecular-weight (LMW) hydrolysates from marine snow. In addition, bin.70 from Bacteroidetes was identified as another crucial bacterium involved in the degradation of marine snow. It predominantly expressed outer membrane receptor proteins (Fig. 5d). Overall, the expression levels of proteins related to chemotaxis, surface attachment, and substrate assimilation shape the metabolic responses of individual taxa to marine snow, thereby providing a molecular basis for microbial niche separation within marine snow.

Discussion

Microbial cleavage of marine snow plays an essential role in the marine carbon cycle. The taxonomic and functional response of the microbial community to marine snow amendment is key to understanding this process. Here, we employed a combined metagenomic and metaproteomic analysis to elucidate the taxonomic and functional aspects of microbial metabolism after marine snow amendment.

Prominent populations promoting the degradation of marine snow

Members of Alteromonadales and Vibrionales became the predominant groups in both FL and MA communities after marine snow amendment (Fig. 1e, f, Supplementary Fig. 5). This finding is consistent with previous studies that have shown a significant increase in the growth of Alteromonadales populations following the addition of high-molecular-weight DOM [80], incubations amended with polysaccharides (such as laminarin) [81], and nutrient addition [82]. Also, it has been reported that members of the Vibrionales are enriched in marine snow, responding to phytoplankton-derived substrates such as low-molecular-weight DOM (LMW-DOM) and iron [15, 31]. It has also been demonstrated that when the concentrations of total organic carbon and nitrogen are very high in the environment, the relative abundance of *Vibrio* increased disproportionately, accounting for more than half of the prokaryotic community [83]. Despite an overall slight decline in the Bacteroidetes population, the relative abundance of a specific member (*Thalassotalea* bin.70) within the Bacteroidetes increased in response to the marine snow addition, particularly in the FL fraction (Fig. 1e, f, Fig. 4, Supplementary Fig. 5, Supplementary Table 6, Supplementary Data 3, Supplementary Data 4). Krüger et al. [35] documented a comparable finding, highlighting the proliferation of only a few free-living Bacteroidetes during the microalgal blooms.

Essential degradation mechanisms in the marine snow culture system

The functional profile of COG categories and KO groups showed significant differences between the metagenomes and metaproteomes (Figs. 1, 2, Supplementary Data 1, Supplementary Data 2). Approximately 38 KO groups involved in the degradation of marine snow were significantly expressed, with their relative abundance in the metaproteomes being one to three orders of magnitude higher than that in the metagenomes (Fig. 2). These observations indicate that the metabolic responses to marine snow addition are more pronounced than the genetic responses. CAZymes are the key enzymes involved in the degradation of algal debris, while TBDTs are responsible for the assimilation of hydrolysates [36, 84]. In our experiment, the relative abundance of CAZymes and TBDTs at both the metagenomic and metaproteomic levels increased after marine snow amendment (Fig. 3g, h, Supplementary Fig. 10, Supplementary Data 5). The diversity (Fig. 3a, b) and variation (Fig. 3c, d) of CAZymes and transporters were lower at the metaproteomic than at the metagenomic level, in contrast to the trends found in the overall taxonomy and function (Fig. 1a, b). These observations can be attributed to Alteromonadales and Chromatiales becoming the major producers of CAZymes (Fig. 3e), and Alteromonadales are the major producers of TBDTs following marine snow amendment (Supplementary Fig. 6b). These results indicate the synergistic expression of key CAZymes and transporters by a few highly abundant species (i.e., Alteromonadales and Chromatiales) was crucial for the degradation of complex carbohydrate polymers, such as marine snow [6–8, 11, 18, 73].

Specifically, AA2 enzymes were predominantly identified in both FL and MA communities (Fig. 3g, Supplementary Fig. 10, Supplementary Table 5, Supplementary Data 5). These enzymes play a crucial role in detoxifying peroxide intermediates generated during the degradation of marine snow due to their high redox potential [78]. Thus, the high relative abundance of periplasmic AA2 indicates their significant involvement in the degradation of phytoplankton-derived marine snow. Additionally, other CAZymes, including AA3_2, AA7, and AA12, identified through different annotation databases were also detected in FL and/or MA communities (Fig. 2, Fig. 3g, Supplementary Table 5, Supplementary Data 2, Supplementary Data 5). These enzymes play a key role in cellulose degradation [85]. Their occurrence further supports the hypothesis that AA enzymes of the CAZyme subfamily are important in the degradation of marine snow. TBDTs were identified as the predominant transporters in both FL and MA communities (Fig. 3h). These findings align with previous studies [33, 34, 36] which also observed a high level of outer membrane TBDT expression during phytoplankton blooms. The most abundant TBDTs identified in our culture system were involved in the uptake of DOM (Fig. 3h, Supplementary Fig. 6d) [9, 73, 86]. A taxonomic analysis at the order level revealed that Alteromonadales were the major contributors to the expression of CAZymes and TBDTs in both the FL and MA communities following marine snow addition (Fig. 3e, Supplementary Fig. 6b). Previous studies have reported similar observations, where Alteromonadales actively secreted extracellular hydrolytic enzymes and responded to variations in organic matter [4, 8, 80, 82]. Also, TBDTs were identified as some of the most abundant transcripts in a DOM-enriched marine microcosm [80]. Previous studies have also indicated that Gammaproteobacteria and Bacteroidetes express TBDTs at high levels, facilitating their acquisition of polymeric matter and other nutrients derived from phytoplankton [9, 62, 87, 88].

In contrast, the relative abundance of ABCTs significantly decreased after the addition of marine snow (Fig. 3h). However, in the FL community, a more diverse range of ABCT subfamilies associated with the transport of amino acids and carbohydrates was found, primarily originating from members of Rhodobacterales and Vibrionales (Supplementary Fig. 11). This suggests that in the ambient water, a wider range of substrates is available for utilization [89–91], likely due to the release of diverse-free enzymes into the ambient seawater during the hydrolysis of marine snow [15, 16, 90]. Previous observations have demonstrated the dominance of the Rhodobacterales taxa, particularly in copiotrophic environments, attributed to their metabolic versatility and adaptability to marine snow facilitated by ABCTs [88, 92, 93].

In addition, the PTS and TRAP-Ts systems were expressed at low abundances in the metaproteomes following the addition of marine snow (Fig. 3h). The PTS is also a crucial transport system for bacterial uptake of various carbohydrates and plays a major role in carbon catabolite repression, an intrinsic substrate preference mechanism in many microorganisms when preferred sugars are scarce [94, 95]. In our marine snow culture system, the low relative abundance of PTS was primarily detected in the FL community due to the likely presence of preferred sugars. TRAP-Ts typically transport C4-dicarboxylates and confer advantages under oligotrophic, deep-sea conditions [9, 62]; hence, they were generally scarce in our culture system.

Identification of key players in the degradation of marine snow

Analysis of the MAGs allows identification of key participants in the degradation of marine snow, while the proteome profile of each MAG unveils distinct cellular responses to the availability of substrates. After the addition of phytoplankton-derived organic matter and the formation of marine snow, members of Gammaproteobacteria, including *Alteromonas* (bin.74), *Thalassotalea* (bin.22), and *Vibrio* (bin.20), exhibited a pronounced increase in abundance within the FL or/and MA fractions compared to the other bins, followed by *Tenacibaculum* (bin.70) from Bacteroidetes in the FL fraction (Fig. 4, Supplementary Data 3, Supplementary Data 4, Supplementary Fig. 9). Overall, this aligns with our analysis that members of Gammaproteobacteria emerged as the the most dominant group at both the metagenomic and metaproteomic level. Compared with the MAGs in the Ocean Microbiomics Database (https://microbiomics.io/ocean/), the MAGs recovered from our research showed relatively low average nucleotide identity (ANI) ($ANI < 97\%$, Supplementary Data 6), indicating their relatively low prevalence in the oligotrophic ocean. This result suggests that the addition of marine snow stimulated the enrichment of a group of bacterial opportunists (especially for bin.74, $ANI = 80\%$), which preferentially take up hydrolysates from marine snow degradation. Furthermore, this is consistent with previous findings indicating that members of Gammaproteobacteria, Bacteroidetes, and Rhodobacteraceae often dominate and synergistically hydrolyze and utilize organic matter from marine snow [96], within the phycosphere [31, 97, 98], during blooms [32, 33], or in diffusion-limited systems [8, 99, 100]. However, other study reported different findings, highlighting Bacteroidetes communities primarily consist of a few proliferating free-living clades during microalgal blooms [35, 101–103]. While these four MAGs exhibited a relatively high abundance, three MAGs, affiliated with Gammaproteobacteria, demonstrated low completeness (Fig. 4, Supplementary Data 3, Supplementary Data 4, Supplementary Data 7). The low completeness might be caused by the high microdiversity within this clade, which coincided with the low prevalence of the three MAGs in the open ocean and their potential as bacterial opportunists for nutrient-rich conditions (Supplementary Data 6). Neverthless, a clear niche separation was observed among these key taxa. The expression profile of the proteome may provide an explanation for such niche separation (Fig. 5). *Alteromonas* bin.74 was the most dominant group in responding to marine snow within our culture system, demonstrating the capability to express secretory AA2 proteins (KatG) related to the detoxification of peroxide intermediates generated during the cleavage of marine snow (Fig. 5a) [78]. Moreover, there was a significant enrichment of various expressed proteins from bin.74, such as iron complex outer membrane receptor protein, OmpA-OmpF porin, and flagellin (Fig. 5a). These proteins primarily facilitate the utilization of preferred substrates in response to changes in substrate composition [4, 31, 80].

The expression profile of *Thalassotalea* bin.22 was largely similar to that of bin.74, except for the AAs proteins (KatG). The absence of CAZymes in bin.22 suggests that *Thalassotalea* members may rely on the breakdown products of marine snow. In addition, the upregulated proteins involved in TonB-dependent receptors, chemotaxis (CheA family), and flagellar proteins in bin.22 after marine snow addition, particularly in the MA (Fig. 5b), may explain why *Thalassotalea* bin.22 is relatively more abundant in the MA than in the FL fraction. In contrast, *Vibrio* bin.20 was preferentially present in the FL fraction because proteins involved in flagella and/or pilus were absent, despite the upregulation of chemotaxis proteins (Fig. 5c). This finding is consistent with previous studies that suggest *Vibrio* thrive primarily on dissolved compounds released by algae, particularly LMW-DOM, preferring a free-living lifestyle, at least temporarily [15, 104, 105]. We speculate that the free-living *Vibrio* bin.20 may be attracted to LMW-DOM-rich hot spots produced by other microorganisms, allowing them to utilize available substrates without incurring unnecessary metabolic costs [106–108]. The relative abundance of Bacteroidetes did not significantly change after the addition of marine snow in both the metagenomes and metaproteomes, except for *Tenacibaculum* bin.70 within Bacteroidetes showing a relatively high abundance in the FL fraction (Fig. 1e, f, Fig. 4, Supplementary Fig. 5, Supplementary Table 6, Supplementary Data 3, Supplementary Data 4). Therefore, *Tenacibaculum* may constitute a group following *Alteromonas* (bin.74), *Thalassotalea* (bin.22), and *Vibrio* (bin.20) in responding to marine snow in our culture system. Furthermore, starch-binding outer membrane proteins (starch utilization system C and D, SusC/SusD) were upregulated in bin.70 following marine snow addition (Fig. 5d). This aligns with previous research indicating that the Bacteroidetes clade possesses a restricted set of conserved polysaccharide utilization loci (PULs, including genes encoding SusC, SusD, and CAZymes), which facilitate the degradation and utilization of algal polysaccharides [35, 109, 110]. It is well known that the degradation of algal polysaccharides produces hundreds of different compounds, including labile, semilabile, and recalcitrant dissolved organic carbon (RDOC) [33, 111, 112]. Therefore, the efficient degradation of marine snow by the specialized prokaryotic consortium not only reflects metabolic activity and characteristics of

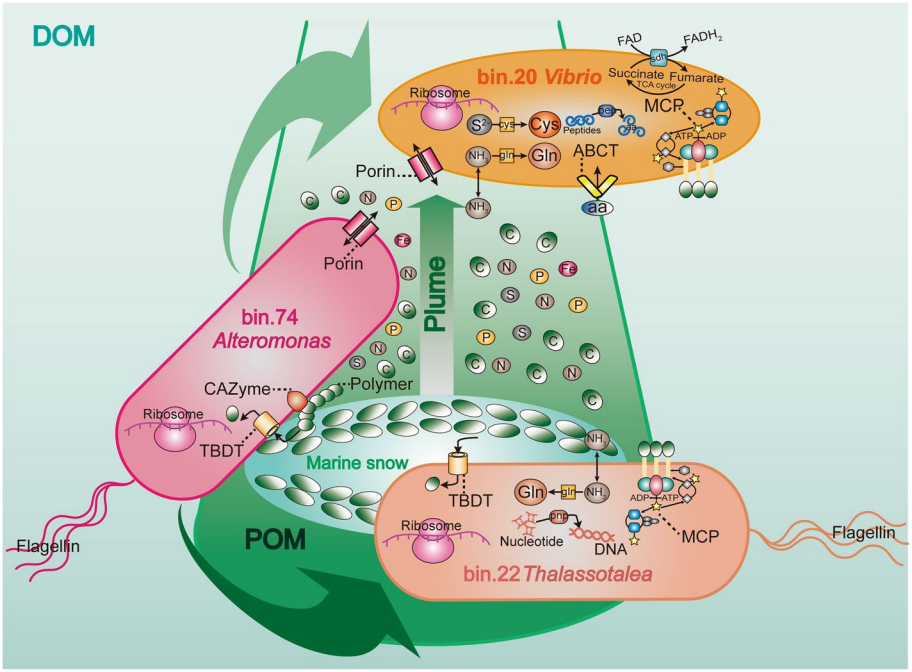

Fig. 6 Schematic diagram illustrating the dominant metabolic processes of the key prokaryotic players in the marine snow culture system. Highly expressed proteins of the top three most abundant MAGs, namely *Alteromonas* (bin.74), *Thalassotalea* (bin.22), and *Vibrio* (bin.20), in marine snow were shown. The relative abundance of expressed proteins in each MAG was larger than or equal to 1% in at least one of the samples. POM, particulate organic matter (i.e., marine snow); DOM, dissolved organic matter; FL, free-living community; MA, marine snow-attached community; MCP, methyl-accepting chemotaxis protein; ABCT, ATP-binding cassette transporters; TBDT, TonB-dependent outer membrane transporter; Gln, glutamine; Cys, cysteine

individual bacterial species but also has the possibility of producing RDOC.

Conclusions

We conducted an experimental investigation of bacterial degradation of marine snow, which was efficiently colonized. We employed metagenomic, metaproteomic, and binning analyses to explore the interactions between prokaryotes and marine snow, uncovering microbial metabolism of the free-living (FL) and marine snow-attached (MA) bacterial consortium. A schematic diagram illustrates the dominant metabolic processes of the key prokaryotic players in marine snow (Fig. 6). In brief, we utilized CAZymes and transporters to gauge the physiological mechanisms involved in degrading and utilizing marine snow, while also examining proteins associated with chemotaxis and BSSs as indicators of survival strategies on marine snow organic matter. Our findings revealed that *Alteromonas* (bin.74) was the dominant group in both the FL and MA communities. *Alteromonas* employ AA2 enzymes of the CAZyme subfamily to detoxify peroxide intermediates generated during the cleavage of marine snow, thereby facilitating their immediate and intact transport into the cells through TBDTs. The released components from marine snow solubilization were preferentially taken up through ABC transporters by *Vibrio* (bin.20), which primarily existed in a free-living lifestyle, and through TBDTs by *Thalassotalea* (bin.22), which primarily adopts a marine snow-attached lifestyle. Therefore, it can be inferred that members of the *Alteromonas* genus are the most dominant microorganisms, likely better adapted to initial degradation of marine snow in both the FL and MA fraction. In contrast, the FL *Vibrio* and MA *Thalassotalea* are more likely utilizing hydrolyzed products, with the former predominantly associated with the FL fraction and the latter primarily associated with the MA fraction [73]. These findings suggest that a few prokaryotic groups, including members of Alteromonadales and Vibrionales, prevailed and became the pivotal drivers in the degradation of marine snow through complementary physiological mechanisms and survival strategies (niche differentiation). These results presented in this study contribute to our understanding of how the synergistic effect of a key prokaryotic consortium influences the fate of marine snow.

Supplementary Information

The online version contains supplementary material available at https://doi.org/10.1186/s40168-025-02097-8.

Supplementary Material 1. Fig. 1 Growth curve of *Picochlorum* sp. Optical density (OD, 550 nm) of *Picochlorum* sp. during incubation. Supplementary Fig. 2 Rolling tank setup and phytoplankton-derived marine snow formation during incubation. The setup consisted of (a) laboratory power supply, (b) a rolling table, and (c) culture bottles placed on the rolling table. (d–f) Marine snow formation during the incubation. Supplementary Fig. 3 Abundance of prokaryotes during incubation. Open circles represent the free-living (size fraction: 0.22–0.8 µm) prokaryotic abundance in the culture group. Closed circles represent the prokaryotic abundance in a given volume of particles (visible to the naked eyes) in the culture group. Open squares represent the prokaryotic cell abundance in the control treatment without the addition of algal organic matter. Supplementary Fig. 4 Variation in the prokaryotic community structure and functional composition in the marine snow microcosm. (a) Community clustering reflected at the gene- and (b) protein level. (c) Functional clusting reflected at the gene- and (d) protein level. Each triangle (Control, C), open square (Free-living, FL), and solid square (Marine snow-attached, MA) represents an individual sample. Roman numerals represent cluster numbers. Percentages indicate Bray–Curtis similarities of community structure or functional classifications. **, $P < 0.01$. Supplementary Fig. 5 Taxonomic and functional profile of free-living (FL) and marine snow-attached (MA) communities in the marine snow culture system. (a) Scatter pie charts showing the compositions and relative abundances of the gene- and (b) protein-based taxonomic contribution to functional classification based on the Clusters of Orthologous Groups (COGs) database at the phylum level (order level for Alpha- and Gammaproteobacteria, and class level for other proteobacteria). C, control prokaryotes. FL, free-living prokaryotes. MA, marine snow-attached prokaryotes. Supplementary Fig. 6 Taxonomic and functional composition of major prokaryotic transporter proteins in each sample. (a) Taxonomic composition of ATP-binding cassette transporters (ABCTs), and (b) TonB-dependent transporters (TBDTs) at the phylum level (order level for Alpha- and Gammaproteobacteria, and class level for other proteobacteria). (c) Functional composition and substrate preference of ABCTs, and (d) TBDTs. C, control; FL, free-living community in the marine snow culture system; MA, marine snow-attached community in the marine snow culture system. Arabic numerals represent replicate numbers. Supplementary Fig. 7 Taxonomic and functional composition of prokaryotic proteins involved in two-component (signal transduction) pathways (TCPs, including histidine kinase, response regulator, and enzymes adapted to changing conditions) and bacterial secretion systems (BSSs) in each sample. (a–e) Taxonomic composition of enzymes associated with various families of TCPs and (f) BSSs at the phylum level (order level for alpha- and gammaproteobacteria, and class level for other proteobacteria). (g–k) Functional composition of enzymes associated with various families of TCPs and (l) BSSs. OmpR, osmolarity response regulator protein R; CitB, response regulator DpiB of citrate/malate metabolism; LytTR, litter; NarL, Nitrate/nitrite response regulator protein L; NtrC, nitrogen regulation protein NR(I); LuxR, Luminescence R; Sec-SRP, general secretory-signal recognition particle; C, control; FL, free-living community in the marine snow micrcosm; MA, marine snow-attached community in the marine snow microcosm. Arabic numerals represent replicate numbers. Supplementary Fig. 8 Mean relative abundance of Gammaproteobacteria in the metagenome and metaproteome at the family level. Members of Alteromonadaceae (order Alteromonadales), Colwelliaceae (order Alteromonadales), and Vibrionaceae (order Vibrionales) are highlighted in orange, purple, and green colors, respectively. All other members are shown in grey scale. Supplementary Fig. 9 Mean relative abundance, calculated as the RPKG of each bin divided by the total RPKG of all bins, of 77 prokaryotic metagenome-assembled genomes (MAGs) classified at the genus level. Relative abundance of prokaryotic MAGs contributing more than 2% in at least one sample are highlighted in different colors, while others are shown in grey. Supplementary Fig. 10 The percentage of prokaryotic carbohydrate-active enzymes (CAZymes) in the metagenome (a) and metaproteome (b) of each sample. AA, Auxiliary activity; CBM, Carbohydrate-binding module; CE, Carbohydrate esterase; GH, Glycoside hydrolase; GT, Glycosyl transferase. C, control; FL, free-living community in the marine snow culture system; MA, marine snow-attached community in the marine snow culture system. Arabic numerals represent replicate numbers. N, not detected. Supplementary Fig. 11 Taxonomic and functional composition of prokaryotic ATP-binding cassette transporter (ABCT) proteins in each sample. (a–c) Taxonomic composition of ABCT subfamilies at the phylum level (order level for Alpha- and Gammaproteobacteria, and class level for other proteobacteria). (d–f) Functional composition and substrate preference of ABCT subfamilies. C, control; FL, free-living community in the marine snow microcosm; MA, marine snow-attached community in the marine snow microcosm. Arabic numerals represent replicate numbers.

Supplementary Material 2. Table 1 Dry biomass concentration of *Picochlorum* sp. in each rolling bottle. Supplementary Table 2 Statistics of proteins identified in the metaproteome. Supplementary Table 3 Alpha-diversity (Shannon index) of taxonomic and functional compositions in the FL and MA communities at both the gene and protein level. Supplementary Table 4 Alpha-diversity (Shannon index) of taxa and functions of CAZymes and transporter proteins in the FL and MA communities at both the gene and protein level. Supplementary Table 5 Relative abundance of CAZymes in the metaproteome. a. Periplasmic CAZymes. b. Cytoplasmic CAZymes. Supplementary Table 6 Percentages of expressed proteins in each bin across samples.

Supplementary Material 3. Data 1: Gene- and protein-based relative abundance in each treatment based on the Clusters of Orthologous Groups (COG) database. Supplementary Data 2. Gene- and protein-based relative abundance in each FL and MA sample based on the KEGG Orthology (KO) database. Supplementary Data 3: Reads per kilobase per genome (RPKG) of prokaryotic metagenome-assembled genomes (MAGs) in each sample. Supplementary Data 4: Relative abundance of prokaryotic MAGs in each sample, calculated as the RPKG of each bin divided by the total RPKG of all bins. Supplementary Data 5: Gene- and protein-based relative abundance in each treatment based on the Carbohydrate-active enzymes (CAZymes) database. Supplementary Data 6: The average nucleotide identity (ANI) values of bin.20, bin.22, bin.70, and bin.77 base on the Ocean Microbiomics database. Supplementary Data 7: Completeness, contamination, GC, size, and N50 of prokaryotic metagenome-assembled genome (MAG) . Supplementary Data 8: Links for each metagenome-assembled genome (MAG) on Figshare.

Acknowledgements

We sincerely thank Prof. Tom Battin and Robert Niederdorfer (Limnology Unit, Dept. Functional and Evolutionary Ecology, University of Vienna) for developing the rolling device. We also thank Chie Amano for her assistance with microscopic counting.

Authors' contributions

G.J.H., Y.Z., and N.J. conceived and designed this study. L.H., Z.Z., and B.S.M. did the experiments, and L.H. and Z.Z. performed the analysis. L.H., Z.Z., Y.Z., and G.J.H. interpreted the data. L.H., Z.Z., and Y.Z. wrote the first draft. All authors discussed the results and contributed to the final version of the paper.

Funding

This work was funded by the National Natural Science Foundation of China (NSFC) projects 42125603, 42430404, and 42421004 to YZ, the NSFC project 42206098 and the National Key Research and Development Program of China (2020YFA0608302) to LH, the Austrian Science Fund (FWF) project I4978-B to GJH, and the MEL Visiting Fellowship MELRS2327 to ZZ.

Data availability

All data used in this study are provided in main text and Supplementary materials. Metagenomic reads are deposited in Natural Center for Biotechnology Information (NCBI), and is available under PRJNA1144259. The sequences of metagenome-assembled genomes (MAGs) are accessible through the link on Figshare (https://figshare.com/s/7aa3c60904aa59d865ae). The mass spectrometry proteomics data have been deposited to the ProteomeXchange Consortium via the PRIDE [113] partner repository with the dataset identifier PXD054591.

Declarations

Ethics approval and consent to participate
Not applicable.

Consent for publication
Not applicable.

Competing interests
The authors declare no competing interests.

Author details
[1]State Key Laboratory of Marine Environmental Science, College of the Environment and Ecology, and College of Ocean and Earth Sciences, Xiamen University, Xiamen, China. [2]Department of Functional and Evolutionary Ecology, University of Vienna, Vienna, Austria. [3]Department of Marine Microbiology and Biogeochemistry, Royal Netherlands Institute for Sea Research (NIOZ), Den Burg, The Netherlands.

Received: 16 August 2024 Accepted: 19 March 2025
Published online: 06 May 2025

References

1. Azam F, Long RA. Sea snow microcosms. Nature. 2001;414:495–8.
2. Karl DM, Lukas R. The Hawaii Ocean Time-series (HOT) program: background, rationale and field implementation. Deep-Sea Res Pt. 1996;II(43):129–56.
3. Arrigo KR. Marine microorganisms and global nutrient cycles. Nature. 2005;437:349–55.
4. Shi Y, Tyson GW, Eppley JM, DeLong EF. Integrated metatranscriptomic and metagenomic analyses of stratified microbial assemblages in the open ocean. ISME J. 2011;5:999–1013.
5. Azam F, Malfatti F. Microbial structuring of marine ecosystems. Nat Rev Microbiol. 2007;5:782–91.
6. Arnosti C. Microbial extracellular enzymes and the marine carbon cycle. Annu Rev Mar Sci. 2011;3:401–25.
7. Kujawinski EB. The impact of microbial metabolism on marine dissolved organic matter. Annu Rev Mar Sci. 2011;3:567–99.
8. Zhao Z, Baltar F, Herndl GJ. Linking extracellular enzymes to phylogeny indicates a predominantly particle-associated lifestyle of deep-sea prokaryotes. Sci Adv. 2020;6: eaaz4354.
9. Bergauer K, Fernandez-Guerra A, Garcia JA, Sprenger RR, Stepanauskas R, Pachiadaki MG, et al. Organic matter processing by microbial communities throughout the Atlantic water column as revealed by metaproteomics. P Natl Acad Sci Usa. 2018;115:E400–8.
10. Tinta T, Zhao Z, Bayer B, Herndl GJ. Jellyfish detritus supports niche partitioning and metabolic interactions among pelagic marine bacteria. Microbiome. 2023;11:156.
11. Arnosti C, Reintjes G, Amann R. A mechanistic microbial underpinning for the size-reactivity continuum of dissolved organic carbon degradation. Mar Chem. 2018;206:93–9.
12. Karner M, Herndl GJ. Extracellular enzymatic activity and secondary production in free-living and marine-snow-associated bacteria. Mar Biol. 1992;113:341–7.
13. Grossart HP, Hietanen S, Ploug H. Microbial dynamics on diatom aggregates in Øresund. Denmark Marine Ecol Progress Series. 2003;249:69–78.
14. Grossart H-P, Tang KW, Kiørboe T, Ploug H. Comparison of cell-specific activity between free-living and attached bacteria using isolates and natural assemblages. FEMS Microbiol Lett. 2007;266(2):194–200.
15. Ziervogel K, Arnosti C. Polysaccharide hydrolysis in aggregates and free enzyme activity in aggregate-free seawater from the north-eastern Gulf of Mexico. Environ Microbiol. 2008;10(2):289–99.
16. Ziervogel K, Steen A, Arnosti C. Changes in the spectrum and rates of extracellular enzyme activities in seawater following aggregate formation. Biogeosciences. 2010;7(3):1007–15.
17. Turner JT. Zooplankton fecal pellets, marine snow and sinking phytoplankton blooms. Aquat Microb Ecol. 2002;27:57–102.
18. Arnosti C, Wietz M, Brinkhoff T, Hehemann J-H, Probandt D, Zeugner L, et al. The biogeochemistry of marine polysaccharides: sources, inventories, and bacterial drivers of the carbohydrate cycle. Annu Rev Mar Sci. 2021;13:81–108.
19. Ivančić I, Paliaga P, Pfannkuchen M, Djakovac T, Najdek M, Steiner P, et al. Seasonal variations in extracellular enzymatic activity in marine snow-associated microbial communities and their impact on the surrounding water. FEMS Microbiol Ecol. 2018;94: fiy198.
20. Steiner PA, Geijo J, Fadeev E, Obiol A, Sintes E, Rattei T, et al. Functional seasonality of free-living and particle-associated prokaryotic communities in the coastal Adriatic Sea. Front Microbiol. 2020;11: 584222.
21. Christina L, Passow U. Factors influencing the sinking of POC and the efficiency of the biological carbon pump. Deep-Sea Res Pt. 2007;II(54):639–58.
22. Buesseler KO, Trull TW, Steinberg DK, Silver MW, Siegel DA, Saitoh S-I, et al. VERTIGO (VERtical Transport In the Global Ocean): a study of particle sources and flux attenuation in the North Pacific. Deep-Sea Res Pt. 2008;II(55):1522–39.
23. Riley J, Sanders R, Marsay C, Le Moigne FA, Achterberg EP, Poulton AJ. The relative contribution of fast and slow sinking particles to ocean carbon export. Global Biogeochem Cy. 2012;26:26.
24. Van der Jagt H, Friese C, Stuut JBW, Fischer G, Iversen MH. The ballasting effect of Saharan dust deposition on aggregate dynamics and carbon export: aggregation, settling, and scavenging potential of marine snow. Limnol Oceanogr. 2018;63:1386–94.
25. Kaltenböck E, Herndl GJ. Ecology of amorphous aggregations (marine snow) in the northern Adriatic Sea. IV. Dissolved nutrients and the autotrophic community associated with marine snow. Mar Ecol-Prog Ser. 1992;87: 147.
26. Müller-MNiklas G, Stefan S, Kaltenböok E, Herndl GJ. Organic content and bacterial metabolism in amorphous aggregations of the northern Adriatic Sea. Limnol Oceanogr. 1994;39:58–68.
27. Vojvoda J, Lamy D, Sintes E, Garcia JA, Turk V, Herndl GJ. Seasonal variation in marine-snow-associated and ambient-water prokaryotic communities in the northern Adriatic Sea. Aquat Microb Ecol. 2014;73:211–24.
28. Salazar G, Cornejo-Castillo FM, Borrull E, Díez-Vives C, Lara E, Vaqué D, et al. Particle-association lifestyle is a phylogenetically conserved trait in bathypelagic prokaryotes. Mol Ecol. 2015;24:5692–706.
29. Mestre M, Borrull E, Sala MM, Gasol JM. Patterns of bacterial diversity in the marine planktonic particulate matter continuum. ISME J. 2017;11:999–1010.
30. Riley GA. Organic aggregates in seawater and the dynamics of their formation and utilization. Limnol Oceanogr. 1963;8:372–81.
31. Raina J-B, Lambert BS, Parks DH, Rinke C, Siboni N, Bramucci A, et al. Chemotaxis shapes the microscale organization of the ocean's microbiome. Nature. 2022;605:132–8.
32. Buchan A, LeCleir GR, Gulvik CA, González JM. Master recyclers: features and functions of bacteria associated with phytoplankton blooms. Nat Rev Microbiol. 2014;12:686–98.
33. Teeling H, Fuchs BM, Becher D, Klockow C, Gardebrecht A, Bennke CM, et al. Substrate-controlled succession of marine bacterioplankton populations induced by a phytoplankton bloom. Science. 2012;336:608–11.
34. Teeling H, Fuchs BM, Bennke CM, Krüger K, Chafee M, Kappelmann L, et al. Recurring patterns in bacterioplankton dynamics during coastal spring algae blooms. Elife. 2016;5: e11888.
35. Krüger K, Chafee M, Ben Francis T, Glavina del Rio T, Becher D, Schweder T, et al. In marine Bacteroidetes the bulk of glycan degradation during algae blooms is mediated by few clades using a restricted set of genes. ISME J. 2019;13:2800–16.
36. Francis TB, Bartosik D, Sura T, Sichert A, Hehemann J-H, Markert S, et al. Changing expression patterns of TonB-dependent transporters suggest shifts in polysaccharide consumption over the course of a spring phytoplankton bloom. ISME J. 2021;15:2336–50.
37. Zhang Y, Jiao N, Sun Z, Hu A, Zheng Q. Phylogenetic diversity of bacterial communities in South China Sea mesoscale cyclonic eddy perturbations. Res Microbiol. 2011;162:320–9.
38. Lu Y, Zhang Y, Wang J, Zhang M, Wu Y, Xiao X, et al. Dynamics in bacterial community affected by mesoscale eddies in the northern slope of the South China Sea. Microb Ecol. 2022;83:823–36.

39. Liang J, Liu J, Zhan Y, Zhou S, Xue C-X, Sun C, et al. Succession of marine bacteria in response to Ulva prolifera-derived dissolved organic matter. Environ Int. 2021;155: 106687.
40. Shanks A, Edmondson E. Laboratory-made artificial marine snow: a biological model of the real thing. Mar Biol. 1989;101:463–70.
41. Guillard RR, Ryther JH. Studies of marine planktonic diatoms: I. Cyclotella nana Hustedt, and Detonula confervacea (Cleve) Gran. Can J Microbiol. 1962;8:229–39.
42. Guillard RR: Culture of phytoplankton for feeding marine invertebrates. In: Culture of marine invertebrate animals: proceedings—1st conference on culture of marine invertebrate animals greenport. Smith WL, Chanley MH, eds. Boston: Springer US; 1975. p. 29–60.
43. Unanue MA, Azúa I, Arrieta JM, Herndl GJ, Iriberri J. Laboratory-made particles as a useful approach to analyse microbial processes in marine macroaggregates. FEMS Microbiol Ecol. 1998;26:325–34.
44. Huang M, He Q, Huang J, Li Z. Research on the rapid determination the biomass of *Chlorella spp*. J Hebe Fish. 2010;4:1–3.
45. Zhu Y, Dunford NT. Growth and biomass characteristics of *Picochlorum oklahomensis* and *Nannochloropsis oculata*. J Am Oil Chem Soc. 2013;90:841–9.
46. Agis M, Unanue M, Iriberri J, Herndl GJ. Bacterial colonization and ectoenzymatic activity in phytoplankton-derived model particles. Part II. Cleavage and uptake of carbohydrates. Microbial ecology. 1998;36:66–74.
47. Besemer K, Singer G, Limberger R, Chlup AK, Hochedlinger G, Hödl I, et al. Biophysical controls on community succession in stream biofilms. Appl Environ Microbiol. 2007;73:4966–74.
48. Besemer K, Singer G, Hödl I, Battin TJ. Bacterial community composition of stream biofilms in spatially variable-flow environments. Appl Environ Microbiol. 2009;75:7189–95.
49. Porter KG, Feig YS. The use of DAPI for identifying and counting aquatic microflora 1. Limnol Oceanogr. 1980;25:943–8.
50. Massana R, DeLong EF, Pedrós-Alió C. A few cosmopolitan phylotypes dominate planktonic archaeal assemblages in widely different oceanic provinces. Appl Environ Microbiol. 2000;66:1777–87.
51. Dong HP, Wang DZ, Dai M, Chan LL, Hong HS. Shotgun proteomics: tools for analysis of marine particulate proteins. Limnol Oceanogr. 2009;7:865–74.
52. Li D, Liu CM, Luo R, Sadakane K, Lam TW. MEGAHIT: an ultra-fast single-node solution for large and complex metagenomics assembly via succinct de Bruijn graph. Bioinformatics. 2015;31:1674–6.
53. Hyatt D, Chen GL, Locascio PF, Land ML, Larimer FW, Hauser LJ. Prodigal: prokaryotic gene recognition and translation initiation site identification. BMC Bioinformatics. 2010;11:119.
54. Li H, Durbin R. Fast and accurate short read alignment with Burrows-Wheeler transform. Bioinformatics. 2009;25:1754–60.
55. Huerta-Cepas J, Szklarczyk D, Heller D, Hernandez-Plaza A, Forslund SK, Cook H, et al. eggNOG 5.0: a hierarchical, functionally and phylogenetically annotated orthology resource based on 5090 organisms and 2502 viruses. Nucleic Acids Res. 2019;47:D309–14.
56. Huerta-Cepas J, Forslund K, Coelho LP, Szklarczyk D, Jensen LJ, von Mering C, et al. Fast genome-wide functional annotation through orthology assignment by eggNOG-mapper. Mol Biol Evol. 2017;34:2115–22.
57. Tatusov RL, Fedorova ND, Jackson JD, Jacobs AR, Kiryutin B, Koonin EV, et al. The COG database: an updated version includes eukaryotes. BMC Bioinformatics. 2003;4:1–14.
58. Kanehisa M, Goto S. KEGG: Kyoto Encyclopedia of Genes and Genomes. Nucleic Acids Res. 2000;28:27–30.
59. Buchfink B, Xie C, Huson DH. Fast and sensitive protein alignment using DIAMOND. Nat Methods. 2015;12:59–60.
60. Zhang H, Yohe T, Huang L, Entwistle S, Wu P, Yang Z, et al. dbCAN2: a meta server for automated carbohydrate-active enzyme annotation. Nucleic Acids Res. 2018;46:W95–101.
61. Petersen TN, Brunak S, Von Heijne G, Nielsen H. SignalP 4.0: discriminating signal peptides from transmembrane regions. Nat Methods. 2011;8:785–6.
62. Tang K, Jiao N, Liu K, Zhang Y, Li S. Distribution and functions of TonB-dependent transporters in marine bacteria and environments: implications for dissolved organic matter utilization. PLoS ONE. 2012;7: e41204.
63. Wu Y-W, Tang Y-H, Tringe SG, Simmons BA, Singer SW. MaxBin: an automated binning method to recover individual genomes from metagenomes using an expectation-maximization algorithm. Microbiome. 2014;2:26.
64. Kang DD, Li F, Kirton E, Thomas A, Egan R, An H, et al. MetaBAT 2: an adaptive binning algorithm for robust and efficient genome reconstruction from metagenome assemblies. PeerJ. 2019;7: e7359.
65. Uritskiy GV, DiRuggiero J, Taylor J. MetaWRAP—a flexible pipeline for genome-resolved metagenomic data analysis. Microbiome. 2018;6:158.
66. Chaumeil P-A, Mussig AJ, Hugenholtz P, Parks DH. GTDB-Tk: a toolkit to classify genomes with the Genome Taxonomy Database. Bioinformatics. 2020;36:1925–7.
67. Stamatakis A. RAxML version 8: a tool for phylogenetic analysis and post-analysis of large phylogenies. Bioinformatics. 2014;30:1312–3.
68. Letunic I, Bork P. Interactive Tree Of Life (iTOL) v4: recent updates and new developments. Nucleic Acids Res. 2019;47:W256–9.
69. Eng JK, McCormack AL, Yates JR. An approach to correlate tandem mass spectral data of peptides with amino acid sequences in a protein database. J Am Soc Mass Spectr. 1994;5:976–89.
70. Elias JE, Gygi SP. Target-decoy search strategy for increased confidence in large-scale protein identifications by mass spectrometry. Nat Methods. 2007;4:207–14.
71. Zhang Y, Wen Z, Washburn MP, Florens L. Improving label-free quantitative proteomics strategies by distributing shared peptides and stabilizing variance. Anal Chem. 2015;87:4749–56.
72. Clarke KR, Gorley RN, Somerfield PJ, Warwick RM. Change in marine communities: an approach to statistical analysis and interpretation. 2014.
73. Zhao Z, Amano C, Reinthaler T, Orellana MV, Herndl GJ. Substrate uptake patterns shape niche separation in marine prokaryotic microbiome. Sci Adv. 2024;10: eadn5143.
74. Kapp K, Schrempf S, Lemberg MK, Dobberstein B. Post-targeting functions of signal peptides. Protein transport into the endoplasmic reticulum. 2009;1:1–16.
75. Laub MT, Goulian M. Specificity in two-component signal transduction pathways. Annu Rev Genet. 2007;41:121–45.
76. Green ER, Mecsas J. Bacterial secretion systems: an overview. In: Virulence mechanisms of bacterial pathogens. Kudva IT, et al, eds. Washington, DC: ASM US; 2016. p. 213–39.
77. Zhao Z, Amano C, Reinthaler T, Baltar F, Orellana MV, Herndl GJ. Metaproteomic analysis decodes trophic interactions of microorganisms in the dark ocean. Nat Commun. 2024;15:6411.
78. Zinser ER. The microbial contribution to reactive oxygen species dynamics in marine ecosystems. Environ Microbiol Rep. 2018;10:412–27.
79. Salah Ud-Din AIM, Roujeinikova A. Methyl-accepting chemotaxis proteins: a core sensing element in prokaryotes and archaea. Cell Mol Life Sci. 2017;74:3293–303.
80. McCarren J, Becker JW, Repeta DJ, Shi Y, Young CR, Malmstrom RR, et al. Microbial community transcriptomes reveal microbes and metabolic pathways associated with dissolved organic matter turnover in the sea. P Natl Acad Sci Usa. 2010;107:16420–7.
81. Reintjes G, Fuchs BM, Amann R, Arnosti C. Extensive microbial processing of polysaccharides in the south pacific gyre via selfish uptake and extracellular hydrolysis. Front Microbiol. 2020;11: 583158.
82. Shi Y, McCarren J, DeLong EF. Transcriptional responses of surface water marine microbial assemblages to deep-sea water amendment. Environ Microbiol. 2012;14:191–206.
83. Gilbert JA, Steele JA, Caporaso JG, Steinbrück L, Reeder J, Temperton B, et al. Defining seasonal marine microbial community dynamics. ISME J. 2012;6:298–308.
84. Bäumgen M, Dutschei T, Bornscheuer UT. Marine polysaccharides: occurrence, enzymatic degradation and utilization. ChemBioChem. 2021;22:2247–56.
85. Schiml VC, Walter JM, Hagen LH, Varnai A, Bergaust LL, De Leon AVP, et al. Microbial consortia driving (ligno) cellulose transformation in agricultural woodchip bioreactors. Appl Environ Microbiol. 2024;90:e01742-24.
86. Chakraborty R, Storey E, van der Helm D. Molecular mechanism of ferricsiderophore passage through the outer membrane receptor proteins of *Escherichia coli*. Biometals. 2007;20:263–74.

87. Dupont CL, Rusch DB, Yooseph S, Lombardo M-J, Alexander Richter R, Valas R, et al. Genomic insights to SAR86, an abundant and uncultivated marine bacterial lineage. ISME J. 2012;6:1186–99.
88. Williams TJ, Long E, Evans F, DeMaere MZ, Lauro FM, Raftery MJ, et al. A metaproteomic assessment of winter and summer bacterioplankton from Antarctic Peninsula coastal surface waters. ISME J. 2012;6:1883–900.
89. Cho BC, Azam F. Major role of bacteria in biogeochemical fluxes in the ocean's interior. Nature. 1988;332:441–3.
90. Smith DC, Simon M, Alldredge AL, Azam F. Intense hydrolytic enzyme activity on marine aggregates and implications for rapid particle dissolution. Nature. 1992;359:139–42.
91. Azam F, Fenchel T, Field JG, Gray JS, Meyer-Reil L-A, Thingstad F. The ecological role of water-column microbes in the sea. Mar Ecol Prog Ser Oldendorf. 1983;10:257–63.
92. Buchan A, González JM, Moran MA. Overview of the marine *Roseobacter* lineage. Appl Environ Microbiol. 2005;71:5665–77.
93. Moran MA, Belas R, Schell M, González J, Sun F, Sun S, et al. Ecological genomics of marine *Roseobacters*. Appl Environ Microbiol. 2007;73:4559–69.
94. Erni B. Glucose transport by the bacterial phosphotransferase system (PTS): an interface between energy-and signal transduction. In: Microbial transport systems. Winkelmann G, eds. Weinheim: Wiley-VCH; 2001. p. 115–38.
95. Deutscher J, Francke C, Postma PW. How phosphotransferase system-related protein phosphorylation regulates carbohydrate metabolism in bacteria. Microbiol Mol Biol R. 2006;70:939–1031.
96. Simon M, Grossart H-P, Schweitzer B, Ploug H. Microbial ecology of organic aggregates in aquatic ecosystems. Aquat Microb Ecol. 2002;28:175–211.
97. Seymour JR, Amin SA, Raina J-B, Stocker R. Zooming in on the phycosphere: the ecological interface for phytoplankton–bacteria relationships. Nat Microbiol. 2017;2:1–12.
98. Zheng Q, Wang Y, Lu J, Lin W, Chen F, Jiao N. Metagenomic and metaproteomic insights into photoautotrophic and heterotrophic interactions in a *Synechococcus* culture. MBio. 2020;11:10–1128.
99. Karl DM, Knauer GA, Martin JH. Downward flux of particulate organic matter in the ocean: a particle decomposition paradox. Nature. 1988;332:438–41.
100. Tamburini C, Garcin J, Grégori G, Leblanc K, Rimmelin P, Kirchman DL. Pressure effects on surface Mediterranean prokaryotes and biogenic silica dissolution during a diatom sinking experiment. Aquat Microb Ecol. 2006;43:267–76.
101. Xing P, Hahnke RL, Unfried F, Markert S, Huang S, Barbeyron T, et al. Niches of two polysaccharide-degrading Polaribacter isolates from the North Sea during a spring diatom bloom. ISME J. 2015;9:1410–22.
102. Kappelmann L, Krüger K, Hehemann J-H, Harder J, Markert S, Unfried F, et al. Polysaccharide utilization loci of North Sea Flavobacteriia as basis for using SusC/D-protein expression for predicting major phytoplankton glycans. ISME J. 2019;13:76–91.
103. Unfried F, Becker S, Robb CS, Hehemann J-H, Markert S, Heiden SE, et al. Adaptive mechanisms that provide competitive advantages to marine bacteroidetes during microalgal blooms. ISME J. 2018;12:2894–906.
104. Mourino-Pérez RR, Worden AZ, Azam F. Growth of Vibrio cholerae O1 in red tide waters off California. Appl Environ Microbiol. 2003;69:6923–31.
105. Takemura AF, Chien DM, Polz MF. Associations and dynamics of Vibrionaceae in the environment, from the genus to the population level. Front Mmicrobiol. 2014;5:75606.
106. Rainey PB, Rainey K. Evolution of cooperation and conflict in experimental bacterial populations. Nature. 2003;425:72–4.
107. Katzianer DS, Wang H, Carey RM, Zhu J. "Quorum non-sensing": social cheating and deception in *Vibrio cholerae*. Appl Environ Microbiol. 2015;81:3856–62.
108. Gauglitz JM, Boiteau RM, McLean C, Babcock-Adams L, McIlvin MR, Moran DM, et al. Dynamic proteome response of a marine *Vibrio* to a gradient of iron and ferrioxamine bioavailability. Mar Chem. 2021;229:103913.
109. Bjursell MK, Martens EC, Gordon JI. Functional genomic and metabolic studies of the adaptations of a prominent adult human gut symbiont, *Bacteroides thetaiotaomicron*, to the suckling period. J Biol Chem. 2006;281:36269–79.
110. Koropatkin NM, Martens EC, Gordon JI, Smith TJ. Starch catabolism by a prominent human gut symbiont is directed by the recognition of amylose helices. Structure. 2008;16:1105–15.
111. Moran MA, Kujawinski EB, Stubbins A, Fatland R, Aluwihare LI, Buchan A, et al. Deciphering ocean carbon in a changing world. P Natl Acad Sci Usa. 2016;113:3143–51.
112. Jiao N, Cai R, Zheng Q, Tang K, Liu J, Jiao F, et al. Unveiling the enigma of refractory carbon in the ocean. Natl Sci Rev. 2018;5:459–63.
113. Perez-Riverol Y, Bai J, Bandla C, García-Seisdedos D, Hewapathirana S, Kamatchinathan S, et al. The PRIDE database resources in 2022: a hub for mass spectrometry-based proteomics evidences. Nucleic Acids Res. 2022;50:D543–52.

Publisher's Note